Concept for a Polarized Electron-Proton Collider with 15–30 GeV c.m. Energy and 10^{33} cm^{-2}s^{-1} Luminosity

I.A. Koop, M.S. Korostelev, I.N. Nesterenko, A.V. Otboev, V.V. Parkhomchuk, E.A. Perevedentsev, V.B. Reva, V.G. Shamovsky, D.N. Shatilov, P.Yu. Shatunov, Yu.M. Shatunov, and A.N. Skrinsky
Budker Institute of Nuclear Physics, Novosibirsk, 630090, Russia
K. D. Jacobs, R. G. Milner, C. Tschalaer, F. Wang, A. Zolfaghari, and G. T. Zwart
MIT-Bates Linear Accelerator Center, Middleton, MA 01949, USA

Abstract

This report presents preliminary results of the feasibility study for a polarized electron-proton beam collider with a center of mass energy range of 15–30 GeV.

1 INTRODUCTION

A ring-ring option for an electron-proton collider with longitudinally polarized particles was investigated in the feasibility study presented below. Objectives of this study are solutions to the physical problems of achieving high luminosity and high polarization of both colliding beams. Electron cooling of the proton beam is essential for the suppression of emittance growth, which results from intra-beam scattering as well as from beam-beam effects. Technical aspects of the discussed facility are the subject of future investigations, but we have tried to stay within realistic constraints based on already achieved parameters of beams and technical components.

2 DESIGN OVERVIEW

Primary performance goals for the collider, based on physics motivations and requirements, are as follows:

- to achieve a peak luminosity of $1 \cdot 10^{33}$ cm^{-2}s^{-1};
- to operate in the energy range $E_{c.m.} = 15$–30 GeV with an energy asymmetry of about 1 to 4, which corresponds to an electron beam energy of $E_e = 3.5$–7 GeV and a proton beam energy of $E_p = 16$–32 GeV;
- to arrange for longitudinal polarization of electrons and protons in two interaction regions with $P \geq 0.5$ and adequate polarization lifetime.

To meet all these requirements we decided on the following key features of the design:

- round beams;
- low $\beta_x = \beta_z$ values at the interaction point;
- head-on collisions;
- multi bunch operation;
- electron cooling of the proton beam at the experimental energy;
- separation of colliding beams by a transverse magnetic field;
- preservation of the proton beam polarization during acceleration by implementing a Siberian Snake scheme in the lattice design;
- possible use of high field polarizing wigglers to increase the self-polarization rate of the electron beam.

A list of the main collider parameters at maximum energy is presented in the Table 1.

Table 1: General parameters of the electron-proton collider.

	Units	Electron ring	Proton ring
Circumference	m	1387.94	1387.35
Energy	GeV	7	32
Arc radius	m	108.50	108.50
Bending radius	m	63.53	63.53
Number of bunches		913	913
Bunch spacing	m	1.52	1.52
Bunch population		$3 \cdot 10^{10}$	$1 \cdot 10^{11}$
Beam currents	A	0.95	3.16
Energy losses/turn	MeV	3.6	
Total radiated power	MW	3.42	
Beam emittances, $\varepsilon_{x,z}$	μm $\cdot$ mrad	46	46
Beta function at IP	cm	10	10
Beam size at IP, $\sigma^*_{x,z}$	μm	68	68
Bunch length, σ_l	cm	10	10
Beam-beam parameter		0.035	0.0023
Lasslett tune shift			0.036
Luminosity	cm^{-2}s^{-1}	$1.0 \cdot 10^{33}$	

3 COLLIDER DESIGN

A layout of the collider is presented in the Fig. 1.

We have chosen a scheme of two rings intersecting in two points. Each ring has two experimental straight sections, two technical straights, and four identical arcs. The rings are separated vertically by about 1 m outside the interaction areas.

The geometry of the interaction regions is dictated by the requirement of preserving the electron beam polarization. So, to provide longitudinal polarization at the collision points, we need to install two spin rotators on both sides of each interaction area. Therefore, asymmetric orbit separation is preferable, because it cancels any spin rotation in the straight.

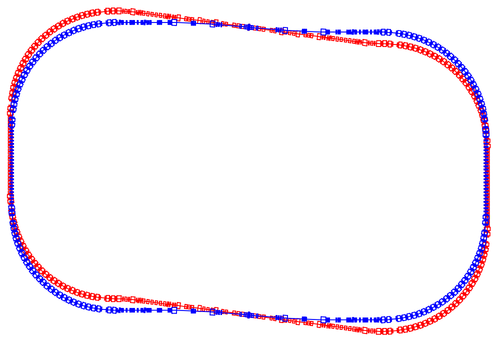

Figure 1: Layout of the e-p collider.

3.1 Electron ring

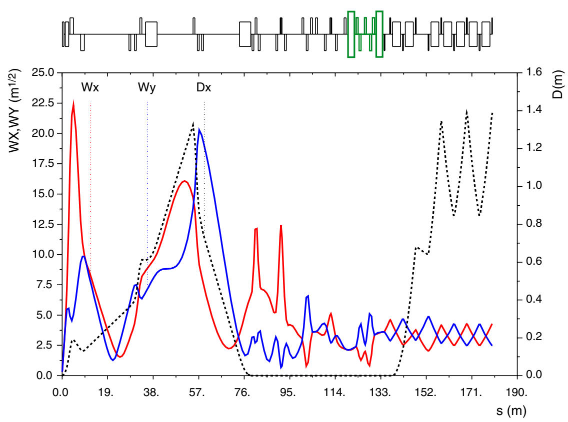

Figure 2: Lattice functions of the electron ring interaction region.

A spin rotation from the vertical direction in the arcs to longitudinal in the IPs is performed in two steps: first, by a solenoidal spin rotator to the horizontal plane and then by dipoles. The $\pm 90^\circ$ spin rotator consists of two superconducting solenoids, each 3 m long, and with fields of about 6 T. Between the solenoids, a focusing structure cancels the betatron coupling and also creates the spin transparency. The solenoids are located in drift spaces, where the velocity vector $\mathbf{v}$ has an angle of $\pm 7.55^\circ$ with respect to the collision axis. (See Fig. 1.) After the solenoids, the spin precesses around the vertical magnetic field, becoming purely longitudinal at the IP, if the electron energy is $E_e = 5.25$ GeV. The last bend is divided into several parts to create an achromat. Two final magnets provide proton and electron separation as close as possible to the IP. On the opposite side of the interaction straight, the spin is restored to the vertical direction by a negative spin rotator. As a result, the spin tune is undisturbed by the interaction region, and the polarization behavior is essentially the same as without the spin rotators. We would like to emphasize that at arbitrary energy the spin is always restored to the vertical direction in the next arc, because of the zero total spin rotation over the interaction straight section.

The lattice of regular FODO cells in the arcs is shown in Fig. 2. The phase advance is 60° in both planes. The total number of cells is 16 per quadrant. The last three cells at the end of each arc function as dispersion suppressors. The arc is terminated by a special quad, which equalizes the vertical and the horizontal amplitude functions, as well as their slopes, at the quad exit.

To compensate for the decrease in proton velocity at lower energies, two bypasses per each quadrant are provided, with each bypass increasing the length of the electron orbit by 15.5 cm. It is possible to activate any number of bypasses to cover a wide range of the proton energies.

3.2 Proton ring

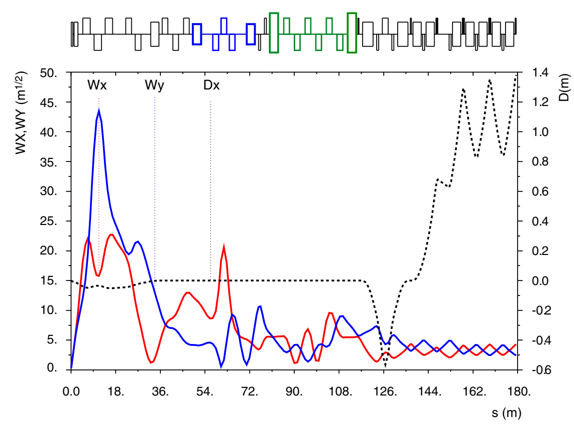

Figure 3: Lattice functions of the proton ring interaction region.

The optical functions of the proton ring are shown in Fig. 3.

The maximum rigidity of the proton ring is 4.598 times higher than the maximum rigidity of the electron ring, and is equal to $BR = 107.362$ T·m. The main dipoles in the arcs, with a field of 1.69 T, have a 63.53 m bending radius. Both rings have the same cell length, $l = 10.652$ m. The only difference is the quadrupole lengths: the proton ring quads are twice as long (0.8 m) as the electron ring quads. The field gradient in these quads is about 25 T/m.

The design of the proton ring interaction region is also driven by the spin manipulation requirements. The straight begins with a spin rotator, which rotates the spin around the longitudinal axis by 90° (if using the full Siberian Snake scheme). The betatron coupling compensation scheme is the same as for the electron beam. The total longitudinal magnetic field integral of the full snake is 120.768 T·m. An antisymmetric lattice after the spin rotator is needed to match the arc optics, provide the low beta function at the IP, and also to provide horizontal orbit bumps.

To bring the beams together, special vertical bridges are placed in the interaction regions between the spin rotators.

4 POLARIZATION ISSUES

The equilibrium polarization direction (vector $\mathbf{n}$) is vertical in the main part of the electron ring and therefore one can expect a relatively low depolarization rate of the electron beam. Moreover, the Sokolov-Ternov polarization mechanism should provide an adequate beam polarization [5]. To minimize the negative effect from spin perturbations $\mathbf{w}$ over the whole straight section, we should fulfill the so-called spin transparency condition:

$$I = \int_{\theta_1}^{\theta_2} \mathbf{w}\boldsymbol{\eta}\, d\theta = 0 \qquad (1)$$

Here $\boldsymbol{\eta} = \boldsymbol{\eta_1} - i\boldsymbol{\eta_2}$ is a complex vector, which is composed of the unity vectors $\boldsymbol{\eta_1}$ and $\boldsymbol{\eta_2}$, which in turn are the two orthogonal solutions of the equation of spin motion for the equilibrium particle [6, 7].

We found a scheme for the focusing structure which contains only regular quadrupoles inside the solenoidal spin rotator and cancels the betatron coupling as well as providing spin transparency. The transfer matrices of a full insertion (from the first solenoid edge to the second solenoid edge) are:

$$T_x = \begin{pmatrix} 0 & -2r \\ (2r)^{-1} & 0 \end{pmatrix}, T_z = \begin{pmatrix} 0 & 2r \\ -(2r)^{-1} & 0 \end{pmatrix} \qquad (2)$$

Here $r = B\rho/B_y$ is the bending radius in the solenoidal field.

Due to the locality of the perturbation, the spin-orbit coupling function does not have a resonant behavior. Loss of polarization from a maximum possible value of $92.4\,\%$ is exclusively caused by the contribution of the wiggling magnets.

Numerical calculations of the radiative polarization in the described electron ring using the ASPIRRIN code [11] show that the reduction of the polarization is of the order of $20\,\%$. See Fig. 4.

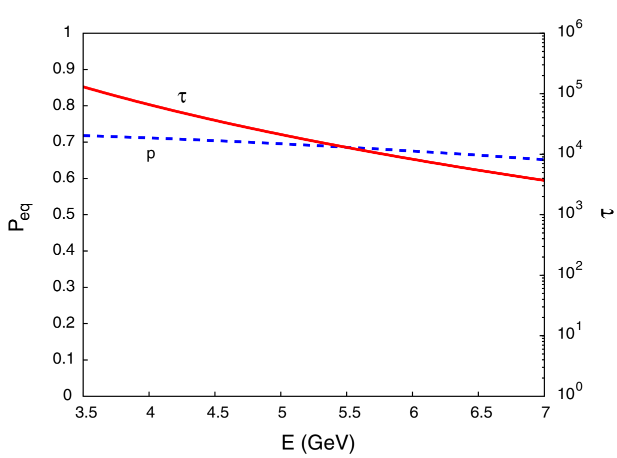

Figure 4: The equilibrium degree of polarization and the spin relaxation time as functions of the electron energy.

These polarization losses can be reduced by a factor of 1.5–2 by higher fields in the arc dipoles or by installation of special polarizing wigglers. Also, in the final design it is reasonable to decrease the field in the wiggling magnets, which are responsible for the loss of polarization.

5 DISCUSSION AND CONCLUSION

In this paper we have not covered injection schemes for either ring. It is clear that the simplest scheme is to inject polarized beams at full energy. On the other hand, the proton ring design allows the possibility of ramping the beam energy without depolarization, because, as an estimate shows, one full Siberian snake is enough to suppress all depolarizing resonances over the entire machine energy range.

The acceleration of the polarized electrons up to the top energy of 7 GeV is questionable. However, the radiative electron polarization can be enhanced considerably by applying special polarizing wigglers with high magnetic field (up to 10 T).

Finally we would like to remark that all values of machine and beam parameters which we used for the design have already been achieved at other storage rings (see for example B-factory status reports) except for the relativistic electron cooling. However, this issue is under investigation at many laboratories (FNAL, BNL). So, we can conclude, that an e-p collider with luminosity $L = 1 \cdot 10^{33}\,\mathrm{cm}^{-2}\mathrm{s}^{-1}$ in the energy range $E_{c.m.} = 15$–30 GeV looks quite realistic.

6 REFERENCES

[1] A. N. Filippov, et al., in *Proceedings of the 15th International Conference on High Energy Accelerators*, 1992, 1145.

[2] I. Nesterenko, et al., in *Proceedings of PAC97*, 1997, 1762.

[3] A. V. Otboyev and E. A. Perevedentsev, in *Proceedings of PAC99*, New York, 1999.

[4] V. V. Parkhomchuk, "New insight in the theory of electron cooling", *NIM* **A441**, 9 (2000).

[5] A. A. Sokolov and I. M. Ternov, *Sov. Phys. Doklady*, **8**, 1203 (1964).

[6] Ya. S. Derbenev, A. M. Kondratenko, and A. N. Skrinsky, *Sov. Phys. Doklady*, **15**, 583 (1970).

[7] Ya. S. Derbenev, A. M. Kondratenko, and A. N. Skrinsky, *Sov. Phys. JETP*, **33**, 658 (1971).

[8] Ya. S. Derbenev and A. M. Kondratenko, *Sov. Phys. JETP*, **35**, 230 (1972).

[9] Ya. S. Derbenev and A. M. Kondratenko, *Sov. Phys. JETP*, **37**, 968 (1973).

[10] Ya. S. Derbenev, A. M. Kondratenko, and A. N. Skrinsky, "Radiative polarization at ultra-high energies", in *Particle Accelerators*, **9**, 247 (1979).

[11] E. A. Perevedentsev, V. I. Ptitsyn, and Yu. M. Shatunov, *Proc. of 5th Int. Workshop on High Energy Spin Physics*, Protvino, 1994, 281.